Characterization of WC-doped NiCrBSi coatings deposited by Laser Cladding; effects of particle size and content of WC powder

Thibaut Perrin, Sofiane Achache, Pierre-Jean Meausoone, Frédéric Sanchette

Characterization of WC-doped NiCrBSi coatings deposited by Laser Cladding; effects of particle size and content of WC powder

Thibaut Perrin[a,b], Sofiane Achache[a,b], Pierre-Jean Meausoone[c], Frederic Sanchette[a,b]

[a]LASMIS, UTT-Université de Technologie de Troyes, Antenne de Nogent, Pôle Technologique de Sud Champagne, 52800 Nogent, France
[b]NICCI, LRC CEA- LASMIS, UTT, Antenne de Nogent, Pôle Technologique de Sud Champagne, 52800 Nogent, France
[c] LERMAB, Université de Lorraine, 27 rue Philippe Séguin CS60036, 88026 Epinal Cedex France

Abstract

Tungsten carbide doped NiCrBSi coatings have been deposited by Laser Cladding (LC) on steel agricultural knives in order to improve their life time. The influence of the mass fraction as well as the particle size of the tungsten carbide powder on structure, microstructure and mechanical properties was analyzed. The mechanical characteristics were studied from micro-hardness tests, pin-on-disc wear tests and cutting tests of plant material. The coating hardness is stable when carbide powder content in the mixture is between 35 and 60 wt%. Then this hardness increases significantly when the carbide content reaches 70 wt%. The wear coefficient in dry conditions decreases when the carbide powder content is increased from 35 to 40 wt%. Further increase of the carbide powder content in the mixture does not affect the wear coefficient. The coating hardness increases with the particle size of the carbide powder. The cutting test shows that the finest particle size (20 - 53 µm) of the carbide powder leads to the lowest values of the cutting-edge wear and the mass loss. This is attributed mainly to the better volume distribution of tungsten carbide particles as well as to the resistance of the matrix due to precipitation of the Ni_4W phase.

Introduction

Cutting tools in agriculture are mainly dedicated to cutting plant materials. They are used for fodder production for animal feed.

These cutting tools are subjected to cyclic mechanical solicitations generated by the shearing of the plant material, which affects the system temperature. This then promotes the phenomena of dry and wet corrosion (depending on the dry matter content) and leads to a complex process of degradation of the tool cutting edge. This degradation can be considered as successive cycles of surface oxidation and removal of this layer by the mechanical action of plant material [1]. This process is particularly affected by the adhesion and cohesion properties of the oxide film. Agricultural cutting tools are frequently submitted to chocks with foreign objects such as stones. Failure of agricultural implements can then occur by bending or by impact [2].

Surface treatments are very widely used on these cutting tools in order to improve resistance to mechanical and thermochemical degradation phenomena.

Surface treatment technologies allow to control the compromise between cost and performance. Many coating technologies exist and they can be distinguished into two families, which are wet deposition and dry deposition. Wet coatings are not discussed as their use for deposition on cutting tools is marginal. Dry coatings are widely used for cutting applications thanks to the large variety of materials, in particular composites and ceramics. These materials, often obtained out of thermodynamic equilibrium conditions, for instance by PVD-arc deposition, have superior properties than those of the materials from which they are derived. They significantly improve the cutting tools resistance and life time.

Spray coatings are widely used for corrosion and / or wear protection applications. Materials are mainly metallic, ceramic or Cermet (CERamic METal) nature. Cermets are generally obtained from mixing carbide or nitride powders with metal matrix powders.
They have been used for many years for anti-wear applications. They are characterized by mixed properties between those of metallic and ceramic coatings. The metal matrix acts as a binder, it promotes adhesion and allows its resistance to impact by plastic deformation. The ceramic particles reinforce the material thanks to their high hardness; they thus lead to a high resistance to wear of the coating. The metal matrix can be elaborated from different alloys (iron, nickel or cobalt base) depending on the application. Cobalt-based alloys (Stellites) are widely used in particular, as a binder in coatings obtained by HVOF with high ceramic

contents (nearly 90%) [3]. They are mainly used for their high corrosion resistance and toughness. Nickel-based self-fusing alloys are those mainly used in composite coatings (Cermets) because of their lower cost than that of Stellites. Their low melting points also facilitate their application by spraying. However, these metallic matrices have a lower corrosion resistance than that of Stellites, which limits their field of application [4]. The most often used ceramic reinforcements are based on carbides because of their very high hardness. Chromium carbides are widely used for anti-wear applications at high temperatures (up to 750 ° C) or in aggressive environments (high corrosion resistance) [5]. Tungsten carbides have a lower maximum service temperature (400 ° C) but their wear resistance is higher. Many studies focus on Cermets NiCrBSi - WC coatings produced by spraying. It appears that the implementation process as well as the composition of the sprayed material have a strong influence on the coating properties, in particular on the tribological behavior [6-7]. This is because the flame-powder spraying technology involves relatively low energies, which would not allow adhesion of a material rich in carbide.

The laser cladding (LC) technology is largely studied because it allows the application of high-quality coatings with high carbide contents, using different matrix [8-11]. The NiCrBSi/WC laser cladded coatings have attracted much attention due to their wear resistance [12-13]. For example, Guo et al. have showed that laser cladded NiCrBSi/WC composite coatings present a very interesting high temperature tribogical behavior, compared to NiCrBSi coating [13].

It should also be noted that this technology has already showed an interesting result for stellite-6-WC coatings, used for protection of agriculture tools [14].

The objective of this study is to develop a high-performance anti-wear laser cladded coating for protection of agricultural cutting tools. The main way to improve mechanical properties of these sprayed coatings is to increase the reinforcement content (tungsten carbide), limited in flame-powder spraying to approximately 30% in mass.

First, the effect of the mass fraction of the tungsten carbide powder mixed with the powder of the NiCrBSi matrix is investigated. Five different mass fractions (35%, 40%, 50%, 60% and 70%) are tested. The WC reinforcement powders have a dense spherical morphology.

The second part of this work deals with the effect of the particle size distribution of tungsten carbide powder. In this case, the mass fraction of WC is fixed at 60% and five particle sizes were selected (20-53µm, 45-90µm, 45-106µm, 45-125µm and 63-150µm).

Experimental details:

Deposition

The powder mixtures are obtained from NiCrBSi matrix powders and tungsten carbide powders. These mixtures are prepared using a KERN PNS 600-3 precision electronic balance (with a capacity of 620 g and a resolution of 0.001 g) to obtain mixtures with tuned WC mass content.

The coatings are deposited by laser cladding using a TrueLaser Robot 5020 robotic reloading cell equipped with a TrueDisk 4001 source, (Nd-YAG solid-state laser with wavelength λ = 1030 nm with a power of 4000 W). The laser power defined during the reloading operations is 800 W for a laser beam diameter of 2.26 mm. Laser reloading is performed by scanning the reloading head at an angle of 5 ° from normal to prevent reflection of laser radiation into the head optics. Successive passes are applied in single passes (so as to limit the local heating of the substrate) with a running speed of 15 mm / s and an overlap of 30% between the passes to ensure continuity of the coating thickness.

Two types of substrates are used in this study. Steel discs are used for physico-chemical, mechanical and tribological analyzes of the coatings. Knives are also used during the cutting tests (see below). These knives are shown Figure 1; The coating is deposited on a 5 mm strip (red arrow in Figure 1) of 12 knives (per powder composition).

The samples were heat-treated after deposition; oil quenching from 1050°C, followed by a tempering at 220°C during 2 hours.

Characterizations

The coatings structure is analyzed by X-ray diffraction (XRD) using a Bruker D8 Advance goniometer. A copper anticathode with a wavelength λ of 1.5418 Å is used for all analyzes. A Hirox S4000 scanning electron microscope was used to characterize the microstructure and Chemical analyzes are performed by energy dispersive X-ray spectroscopy (EDS). Hardness is first measured on the NiCrBSi matrix and tungsten carbide reinforcements. The coating hardness is then evaluated using a higher test load. A Vickers Q10CHD Master (QNESS) microdurometer with motorized X, Y and Z axis is used; the load can vary within a range of values between 50 g and 10 kg. Hardness measurements are performed on the surface of coated, heat-treated, ground and mirror-polished pins.

The pion-on-disc tribological tests are carried out on a high temperature tribometer (CSM) with the following experimental conditions:

- Radius of the friction track: 6.00 mm.
- Linear speed: 100 mm / s.
- Load: 10 N.
- Counter body: 6 mm diameter grade 24 alumina (Al2O3) ball (1500 HV10).
- Data acquisition frequency: 7.5 Hz.
- Friction distance: 10,000 m
- Temperature: 23 ± 2 ° C.
- Hygrometry: 40 ± 10%.
- Atmospheric pressure.

A first series of tests is carried out without lubrication, it is called "dry conditions". Its purpose is to assess the resistance of coatings under standard operating conditions as the process of cutting dry plant material like hay.

A second series of tests is carried out under lubrication, it is called "wet conditions". The goal is then to evaluate the effect of lubrication on the friction properties of the coatings. This series of tests can be compared to the process of cutting fresh plant material such as alfalfa (intended for silage production after dehydration). The lubricating solution used is produced from an infusion of dehydrated alfalfa in deionized water; it is hereinafter called "alfalfa solution".

Alfalfa solution is obtained according to the following protocol:
- Weighing of 100 g of dehydrated alfalfa (Rumiluz).
- Mix in a bottle and macerate for 96 hours in 2 L of demineralized water.
- Filtration of the solution.
- Store in an airtight bottle protected from light.

The pH of the alfalfa solution, measured using a HI 83141 pH meter (Hanna), decreases slightly when infusing dehydrated alfalfa between 0 and 96 hours. It is measured at 5.49, this slightly acidic value is consistent with that of lightly fermented plant material for forage production.

The wear coefficients are evaluated using an AltiSurf 500 confocal laser profilometer (Altimet), equipped with a CL2 probe (400). A scan of the friction track is performed on a 2 x 3 mm area.

The cutting test is used to machine compressed straw panels in order to simulate the process of cutting plant material [15]. This cutting test was also used by Guillaume Simonin [16]. The

advantage of using this type of panel is its manufacturing process by hot pressing without chemical binder, as in the work of Wang et al. [17]. These panels, normally intended for insulation applications, measure 2500 x 1200 x 58 mm and have an average density of 22 kg / m². In order to be able to be handled by the cutting test machine, these panels are cut into 15 small panels of 500 x 300 x 58 mm.

Results and discussion

1: Effect of the mass fraction of WC reinforcement in NiCrBSi matrix

As already specified, the effect of the mass fraction of the tungsten carbide powder mixed with the powder of the NiCrBSi matrix is investigated. Five different mass fractions (35%, 40%, 50%, 60% and 70%) are tested. The WC reinforcement powders have a dense spherical morphology.

1 .1 Structure

When increasing the mass content of tungsten carbide powder in the powder mixture deposited by LC, there is a shift of the diffraction peaks of the main phase Ni_3Fe of the matrix (Figure 2). The main diffraction peaks of this phase (Figure 2b), shows that, when the tungsten carbide powder content increases in the powder's mixture, the reflections (111), (200), (311) of this phase shift towards the small angles until the diffraction peaks can be indexed in the NiFe phase. This means an iron enrichment, which favors the NiFe phase, related to the substrate dilution.

The substrate dilution rate can be qualitatively estimated from equation (1) as shown in Figure 3. Values were determined by image analysis via ImageJ. The substrate dilution rate as well as of the iron content of the NiCrBSi matrix increase when tungsten carbide powder content increases (Figure 4). The nominal iron content of the matrix powder is 2.8 wt%, the substrate dilution is therefore a major phenomenon. Optimizing the LC deposition parameters would minimize this effect.

Previous studies [18-19] on LC process parameters have shown that too much power and too low powder flow rate lead to dilution of the substrate. Thus, the iron enrichment of the main phase of the matrix can be attributed to the increase in the size of the molten bath at the surface of the substrate, due to the reduction in the quantity of matrix to be fused associated with the increase in the mass fraction of tungsten carbide in the powder mixture.

As expected, when the mass fraction of tungsten carbide increases, the intensity of the WC and W_2C carbides diffraction peaks increases, while that of the main phase of the matrix decreases (Figure 2a). The W_2C / WC molar ratio (not shown), calculated from the proportion of the WC and W_2C phases estimated via DiffractEva softwear, increases linearly as a function of the mass fraction of tungsten carbide. The diffusion of carbon from WC is favored. This is attributed to the increase in the amount of radiated energy dissipated to the tungsten carbide particles due to the reduction in the amount of matrix in the initial powder mixture. The growth of the Ni_4W phase is also favored by the increase of the carbide content which is consistent with the increase in the carbide - matrix interface density.

1.2 Microstructure

Figure 5 shows the cross-section images of the deposited coatings as a function of tungsten carbide content. Contrary to observations of Garcia et al [12], the distribution of the carbide particles appears to be homogeneous from interface to the coating surface, which can be attributed to the lower ticknesses studied in our case. Some cracks can be observed (figure 5d). Laser cladding technique is associated with rapid heating and solidification, induced residual stress during laser cladding could lead to crack formation in the coating. [20-22].

1.3 Mechanical properties

1.3.1 Hardness and wear

Figure 6 shows the evolutions of the matrix, coating and tungsten carbide hardness as a function of tungsten carbide content. Even the increase of W_2C fraction with tungsten carbide increase (detected by XRD), the tungsten carbide hardness remains constant (red curve figure 6).

The NiCrBSi matrix shows a stable hardness value between 35 and 60 wt% of carbide powder before increasing significantly when the carbide powder content reaches 70 wt% (blue curve in Figure 6). This result can be correlated with the dilution of the substrate, which stabilizes after 60 wt% of carbide powder. The progressive iron enrichment of the NiCrBSi matrix does not induce a significant variation in its hardness, contrary to the result of Sousa et al [23]. The hardening of the matrix observed when the carbide powder content reaches 70 wt% can be explained by the WC decomposition. The precipitation of the Ni_4W phase is then favored, leading to the matrix hardening, because of the increase in the matrix-carbide interfacial surface.

Coating hardness (green curve in Figure 6) follows the same trend as the matrix hardness; its value is stable between 35 and 60 wt% of carbide powder content and increases at 70 wt%. This result is again attributed to the substrate dilution, which limits the volume density of reinforcement in the deposit between 35 and 60 wt%. As the matrix - carbide interface density does not vary significantly, the precipitation of Ni_4W in the matrix is limited. These two phenomena explain the stabilization of the coating hardness. At 70 wt% of carbide powder content, the substrate dilution becomes limited. Thus, the carbide volume density is higher, which favors the matrix - carbide interface density associated with the precipitation of Ni_4W.

The Friction coefficient in wet conditions is in the range 0.12 to 0.20 whereas it is between 0.70 and 0.82 in dry condition. The alfalfa solution plays a lubricating role. Consequently, a significant decrease in the average wear coefficient, compared to those measured in dry conditions, is also measured. Anyway, no clear or significant effect of the tungsten carbide content is observed. Nevertheless, a slight tendency toward an increase of the friction coefficient with tungsten carbide content increase can be observed. The same tendency was observed by Garcia et al. [12]. It was attributed to the progressive change of the predominant wear mechanism from adhesive–oxidative to abrasive.

The wear coefficient in dry conditions decreases from $1.6.10^{-6}$ mm^3/J to $6.4.10^{-7}$ mm^3/J when the tungsten carbide content increases from 35 to 40 wt% and stabilizes above. Van Acker et al. [24] showed a sharp decrease in the wear coefficient when increasing the carbide content between 0 and 50 vol%. The wear improvement was expected and consistent with the addition of a hard phase.

1.3.2 Cutting test

Improvement of cutting performance of a coating by increasing its tungsten carbide content from 35 to 50 and 60 wt% is shown Figure 7. It is necessary to increase the tungsten carbide powder content from 35 up to 50 wt% in order to obtain a gain on edge resistance as well as on the mass loss of 27% and 24% respectively. This result is consistent with the decrease of the friction coefficient in dry conditions (previous section, 1.3.1).

The wear of the matrix as well as the loss of the reinforcements are the two main parameters responsible for the wear of these composite layers. Thus, the improvement in wear resistance from 35 wt% carbide could be explained by (i) decrease in matrix volume and (ii) matrix hardening.

2. Effect of the particle size of WC reinforcements

This section deals with the effect of the particle size of tungsten carbide particles on the structural, microstructural and mechanical properties of coatings obtained by LC. The tungsten carbide powder used has a WC bulk density of 9.9 g / cm^3. The mixture consists in 60 wt% WC with NiCrBSi matrix (11 wt% Cr). In this case, five particle sizes were selected (20-53µm, 45-90µm, 45-106µm, 45-125µm and 63-150µm).

2.1 Structure

Figure 8 shows the decrease in the intensity of the (121) Ni_4W diffraction peak (2θ= 43.5°) when the particle size of the tungsten carbide powder increases. This suggests that the decomposition of WC is favored by a fine particle size of the tungsten carbide particles. Indeed, this phenomenon can be correlated with the increase of matrix – carbide interface area induced by the decrease in the particle size of the carbide powder. The diffusion of carbon from the WC phase is then promoted thanks to the exchange surface between the heated matrix and the tungsten carbide grains.

The W_2C / WC molar ratio (calculated from phase quantification on DiffractEva) tends to decrease from 0.35 to 0.31with increasing particle size of the tungsten carbide powder in the range 20-53µm to 63-150µm. This confirms that a fine particle size of the tungsten carbide powder promotes its decomposition as observed by Van Acker et al. [24]. However, the finest particle size (20 - 53 µm) shows a proportion of the W_2C phase equivalent to that of the particle size (45 - 106 µm). Coupling this observation with the significant precipitation of the Ni_4W phase, this suggests that the dissolution of WC during the heat treatment in the case of the finest particle size is a major phenomenon.

2.2 Microstructure

SEM micrographs (Figure 9) shows a grey phase observed in the matrix from the interface with the tungsten carbide grains. This phase appears clearly in the case of the finest particle size (figure 9.a) of tungsten carbide powder (20 - 53 µm). This grey phase is attenuated to become negligible in the case of the coarser particle size (63 - 150 µm) (Figure 9.d). The degree and mechanisms of WC particles heat damage are related to their size [25]. This degree is larger where their radius is smaller, due to their higher solubility. The heat damage mechanisms of WC particles have been well explained by Wang et al. [new ref]. According to the size and the different heat process of WC particles, three heat damage modes could

occur, i.e: (1) The dissolution-diffusion controlled heat damage, (2) the collapsibility-dissolution-diffusion controlled heat damage and (3) the dissolution-precipitation controlled heat damage.

Firstly, WC particles present the mechanism of the dissolution-diffusion controlled heat damage: the edge of WC particle dissolve into the NiCrBSi matrix, and the alloy elements such as Ni, Cr and Si from the NiCrBSi matrix diffuse into WC particle, resulting in the formation of the alloyed reaction layer. Secondly, WC particles presents the collapsibility-dissolution-diffusion controlled heat damage: some WC particles with a relatively larger size are broken into small pieces that are alloyed completely to form the phases containing a relatively higher W content. Thirdly, WC particles present the mechanism of the dissolution-precipitation controlled heat damage: some WC particles with a relatively smaller size are broken into smaller pieces that are dissolved completely into the NiCrBSi matrix, resulting in the precipitation of the different phases with different morphologies. This last mechanism could be predominant in the case of the finest particle size (Figure 9.a) and it is clearly shown that the degree of particles heat damages is low for higher particle size (Figure 9.b to 9.d).

The chemical composition maps (not shown) indicates that the grey phase is rich in nickel and tungsten, which tends to confirm the hypothesis of Ni_4W precipitation favored by W_2C decomposition, more particularly in the case of a fine particle size of the tungsten carbide powder.

2.3 Mechanical properties

2.3.1 Hardness and pin-on-disc

Evolution of the particle size of the tungsten carbide powder does not show a significant effect on carbides hardness (red curve in Figure 10). The decomposition of carbides and the precipitation of W_2C at the matrix-carbides interface, taking place at the periphery of the grains, therefore does not affect their intrinsic hardness. The NiCrBSi matrix shows a higher value in the case of the finest particle size (blue curve Figure 10). This result is again attributed to the decomposition of tungsten carbides at matrix - carbide interfaces. The precipitation of the Ni_4W phase is promoted in the NiCrBSi matrix, which improves its hardness as shown by Liyanage et al [26].

The coating hardness increases with the particle size of the carbide powder (green curve Figure 10). The W_2C phase at the periphery of the grains weakens the interfaces, which leads

to cracks under the effect of stress (purple arrows in Figure 11.a). In addition, the cracking of the NiCrBSi matrix appears under the effect of its plastic deformation (blue arrows Figure 11.a). This tends to show that Ni_4W precipitates in the matrix seems to reduce its shear strength. In the case of the largest particle size (Figure 11.b), the interfaces and the matrix are clearly less sensitive to cracking, which explains the higher coating hardness.

Pin-on-disc tests in dry and wet conditions showed that the finest particle of the tungsten carbide powder improves slightly the wear coefficient whereas the friction coefficient seems to be not affected (not shown). This behavior was also observed by Deschuyteneer zt al. [27]. Van Acker et al [14] showed that a small particle size powder significantly improves the coating resistance for low carbide contents. When this becomes significant (50% in volume), the effect becomes negligible. The non-significant results, in our case, can therefore be attributed to the high tungsten carbide density of our coatings. The 10 N test load does not appear to be sufficient to discriminate coatings with such reinforcing concentrations.

2.3.2 Cutting test

The 45 - 106 µm particle size of the tungsten carbide powder leads to the highest cutting-edge wear (Figure 20). The finest particle size (20 - 53 µm) leads to the lowest values measured in terms of the cutting-edge wear rate and mass loss. These interesting values, with small grain size, can be attributed to several effects: i) The small size of the particles improves their volume distribution in the coating, ii) The mass loss associated with the pulling out of the carbides increases with the particle size of the tungsten carbide powder, iii) The higher hardness of the NiCrBSi matrix, due to the precipitation of Ni_4W, improves its resistance.

Conclusion

Tungsten carbide doped NiCrBSi coatings have been deposited by Laser Cladding (LC). The influence of the mass fraction as well as the particle size of the tungsten carbide powder on the structure, microstructure and mechanical properties was analyzed. The mechanical characteristics were studied from micro-hardness tests, pin-on-disc wear tests and cutting tests of plant material.

Increase in the mass fraction of the tungsten carbide powder leads to an iron enrichment of the NiCrBSi matrix, which favors NiFe at the expense of Ni_3Fe, due to the increase in the dilution

rate of the substrate. The W_2C / WC molar ratio increases as a function of the tungsten carbide powder content. The coating hardness is stable when carbide powder content in the mixture is between 35 and 60 wt%. Then this hardness increases significantly up to 840 HV_{10} when the carbide content reaches 70 wt%. The wear coefficient in dry conditions decreases when the carbide powder content is increased from 35 to 40 wt%. Further increase of the carbide powder content in the mixture does not affect the wear coefficient. Concerning plant cutting, it is necessary to increase the tungsten carbide powder content from 35 up to 50 wt% in order to obtain a gain of the knive's cutting-edge resistance as well as of the mass loss of 27% and 24% respectively.

The coating hardness increases from 585 HV_{10} to 730 HV_{10} with the particle size of the carbide powder whereas the cutting test shows that the finest particle size (20 - 53 µm) of the carbide powder leads to the lowest values of the knive's cutting-edge wear and the mass loss. This can be attributed mainly to the better volume distribution of tungsten carbide particles as well as to the resistance of the matrix due to precipitation of the Ni_4W phase.

References

[1] Z. Dadić, Tribological principles and measures to reduce cutting tools wear, International conference "Mechanical Technologies and Structural Materials" Split, ISSN 1847-7917 MTSM2013 26-27.09.2013

[2] T. Rostek et W. Homberg, Grading technologies for the manufacture of innovative cutting blades, Palermo, Italy, 2018, p. 100013, doi: 10.1063/1.503495III.

[3] M. S. Lamana, A. G. M. Pukasiewicz, et S. Sampath, « Influence of cobalt content and HVOF deposition process on the cavitation erosion resistance of WC-Co coatings », Wear, vol. 398-399, p. 209-219, mars 2018, doi: 10.1016/j.wear.2017.12.009.

[4] P. Houlle, Résistance à la corrosion aqueuse des alliages de nickel, Techniques de l'Ingénieur, Réf : COR312 v1, 2015

[5] A. Wank, B. Wielage, G. Reisel, T. Grund, et E. Friesen, Performance of thermal spray coatings under dry abrasive wear conditions, The coatings 2004

[6] A. Mate et H. Deore, Review Paper on Effect of WC-Ni Content on Wear Behavior of Laser clad Ni- based alloys, vol. 5, no 6, p. 11, 2017.

[7] R. Seger, Effect of tungsten carbides properties of overlay welded WC/NiSiB composite coatings, 2013, p. 64.

[8] S. Zhou, X. Dai, H. Zheng, Microstructure and wear resistance of Fe-based WC coating by multi-track overlapping laser induction hybrid rapid cladding
Opt. Laser Technol., 44 (2012), pp. 190-197

[9] S. Zhou, Y. Huang, X. Zeng, A study of Ni-based WC composite coatings by laser induction hybrid rapid cladding with elliptical spot
Appl. Surf. Sci., 254 (2008), pp. 3110-3119

[10] S.M. Zhu, Y.D. Zhang, The microstructure and wear-resistant properties of laser cladding Ni-based WC alloy on Q345 steel surface
Appl. Mech. Mater., 556–562 (2014), pp. 189-192

[11] W.C. Lin, C. Chen, Characteristics of thin surface layers of cobalt-based alloys deposited by laser cladding
Surf. Coat. Technol., 200 (2006), pp. 4557-4563

[12] A. García, M. R. Fernández, J. M. Cuetos, R. González, A. Ortiz, M. Cadenas. Study of the sliding wear and friction behavior of WC+NiCrBSi laser cladding coatings as a function

of actual concentration of WC reinforcement particles in ball on disk test. Tribol Lett. (2016) 63:41.

[13] C. Guo, J. Zhou, J. Chen, J. Zhao, Y. Yu, H. Zhou. High temperature wear resistance of laser cladding NiCrBSi and NiCrBSi/WC-Ni composite coatings. Wear 270 (2011) 492-498.

[14] D. Bartkowski, A. Bartkowska. Wear resistance in the soil of Stellite-6/WC coatings produced using laser cladding method; International Journal of Refractory Metals and Hard Materials. 64 (2017), Pp 20-26

[15] M. Gauvent, Optimisation de la durée de vie d'un outil de coupe pour l'industrie du bois. Analyse et compréhension des modes d'usure. Mise au point de solutions innovantes avec tests industriels, Thèse de l'Université Henri Pointcarré, Nancy I, 2006.
[16] G. Simonin, Améliorations des performances d'outils de coupe pour la première transformation du bois, Thèse de l'Université Henri Pointcarré, Nancy I, 2010.

[17] J. Wang, B. Wang, J. Liu, L. Ni, et J. Li, « Effect of Hot-Pressing Temperature on Characteristics of Straw-Based Binderless Fiberboards with Pulping Effluent », Materials (Basel), vol. 12, no 6, mars 2019, doi: 10.3390/ma12060922.

[18] A. Gowtham, G. Chaitanya, J. K. Katiyar, A. Chandak, et T. V. K. Gupta, « Experimental investigations on laser cladding of NiCrBSi + WC coating on SS410 », Materials Today: Proceedings, oct. 2019, doi: 10.1016/j.matpr.2019.09.044.

[19] D. Tanigawa et al., « Suppression of dilution in Ni-Cr-Si-B alloy cladding layer by controlling diode laser beam profile », Optics & Laser Technology, vol. 99, p. 326-332, févr. 2018, doi: 10.1016/j.optlastec.2017.09.019.

[20] Alidokht, S.A.; Yue, S.; Chromik, R.R. Effect of WC morphology on dry sliding wear behavior of cold-sprayed Ni-WC composite coatings. Surf. Coat. Technol. 2019, 357, 849–863.

[21] Chong, P.; Man, H.; Yue, T. Microstructure and wear properties of laser surface-cladded Mo-WC MMC on AA6061 aluminum alloy. Surf. Coat. Technol. 2001, 145, 51–59.

[22] Pengxian Zhang , Yibin Pang, Mingwei Yu, Effects of WC Particle Types on the Microstructures and Properties of WC-Reinforced Ni60 Composite Coatings Produced by Laser Cladding. Metals. 2019, 9, 583.

[23] J. M. S. de Sousa, F. Ratusznei, M. Pereira, R. de M. Castro, et E. I. M. Curi, « Abrasion resistance of Ni-Cr-B-Si coating deposited by laser cladding process », Tribology International, vol. 143, p. 106002, mars 2020, doi: 10.1016/j.triboint.2019.106002.

[24] K. Van Acker, D. Vanhoyweghen, R. Persoons, et J. Vangrunderbeek, « Influence of tungsten carbide particle size and distribution on the wear resistance of laser clad WC/Ni coatings », Wear, vol. 258, no 1, p. 194-202, janv. 2005, doi: 10.1016/j.wear.2004.09.041.

[25] X. Wang, S. Zhou, X. Dai, J. Lei, J. Guo, Z. Gu, T. Wang, «Evaluation and mechanisms on heat damage of WC particles in Ni60/WC composite coatings by laser induction hybrid cladding», International Journal of Refractory Metals and Hard Materials, Vol. 64, April 2017, Pages 234-241

[26] T. Liyanage, G. Fisher, et A. P. Gerlich, « Influence of alloy chemistry on microstructure and properties in NiCrBSi overlay coatings deposited by plasma transferred arc welding (PTAW) », Surface and Coatings Technology, vol. 205, no 3, p. 759-765, oct. 2010, doi: 10.1016/j.surfcoat.2010.07.095

[27] D. Deschuyteneer, F. Petit, M. Gonon, F. Cambier. Processing and characterization of laser clad NiCrBSi/WC composite coatings — influence of microstructure on hardness and wear. Surf. Coat. Technol., 283 (2015), pp. 162-171

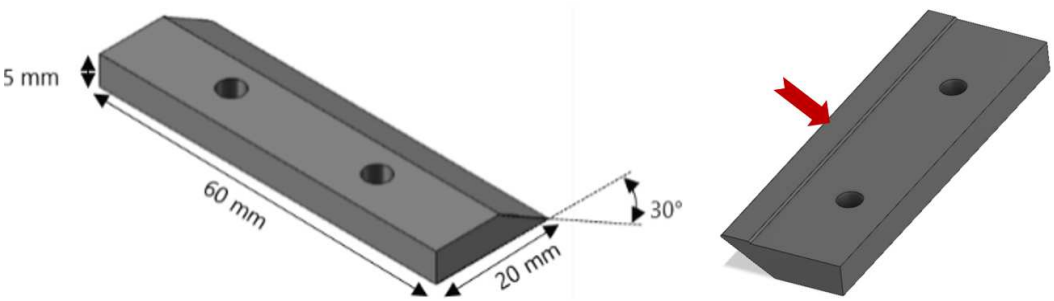

Figure 1: Geometry of the knives used for the cutting tests.

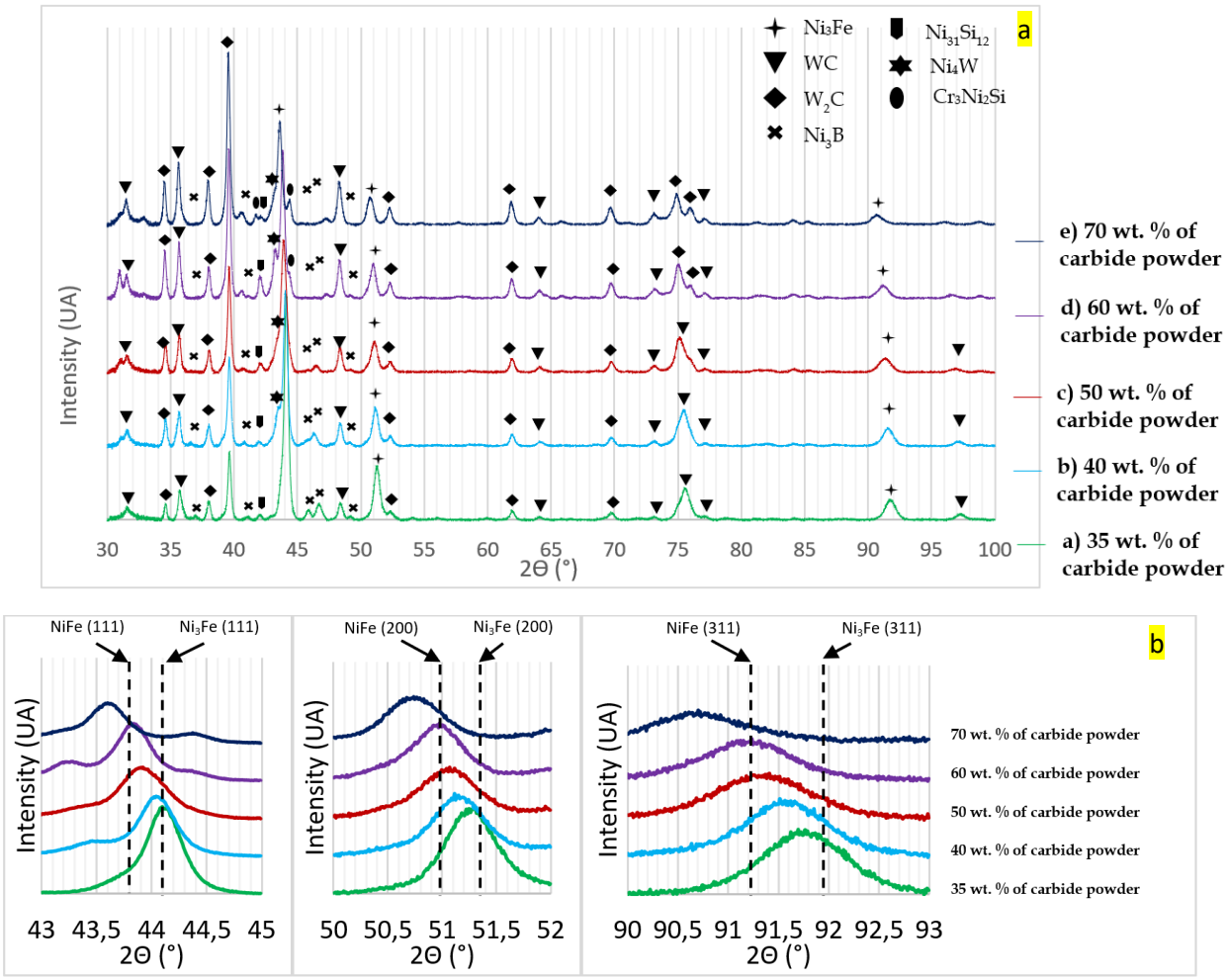

Figure 2: a) Diffractograms of LC coatings deposited with different contents of WC mixed with the NiCrBSi matrix (11wt% of chromium): 35wt%, 40wt%, 60wt% and 70wt%. b) Detailed view of the diffraction peaks corresponding to the main phase of the matrix over the 2Θ diffraction ranges a) 43 - 45 ° (110), b) 50 - 52 ° (200) and c) 90 - 93 ° (311) during the variation of the mass content of tungsten carbide powder mixed with the NiCrBSi matrix (11wt% Cr).

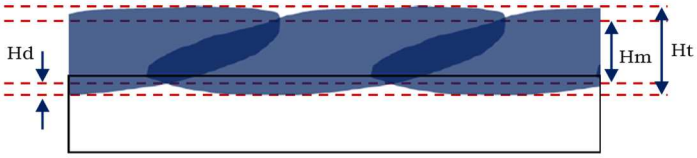

$$D = \frac{Hd}{Ht} \, x \, 100 \qquad (1)$$

Figure 3: Evaluation method of the substrate dilution for coatings deposited by LC with: D = dilution rate (%), Ht = total thickness (µm), Hm = minimum coating thickness (µm) and Hd = dilution thickness of the substrate (µm) [11].

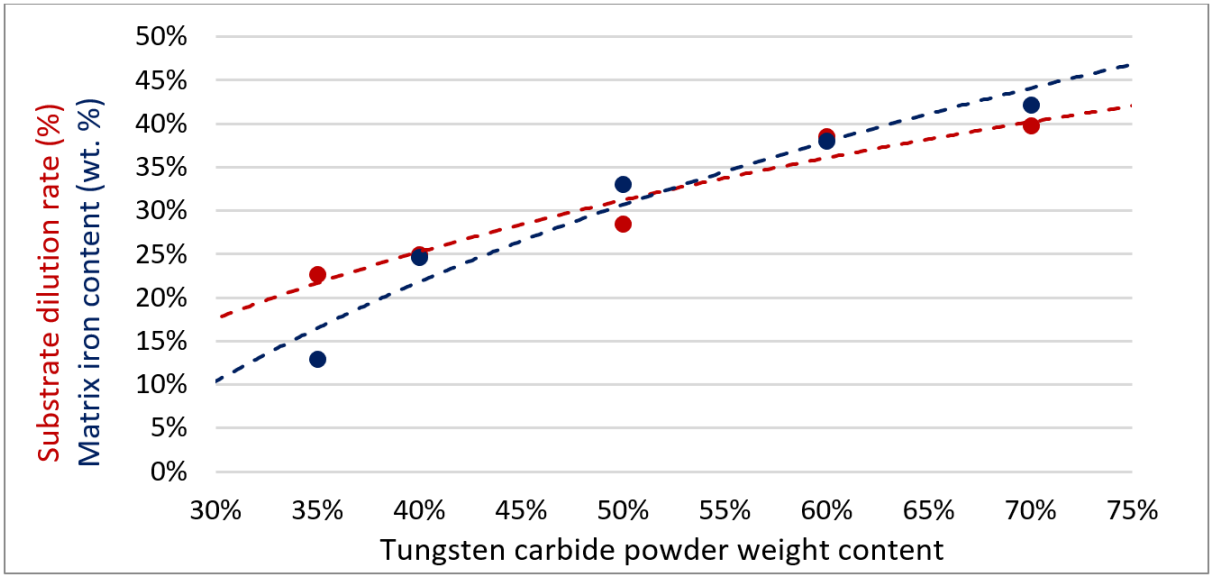

Figure 4: Evolution of iron content of NiCrBSi matrix and substrate dilution rate as a function of the substrate dilution rate when fraction of WC carbide powder increases in the powder mixture deposited by LC.

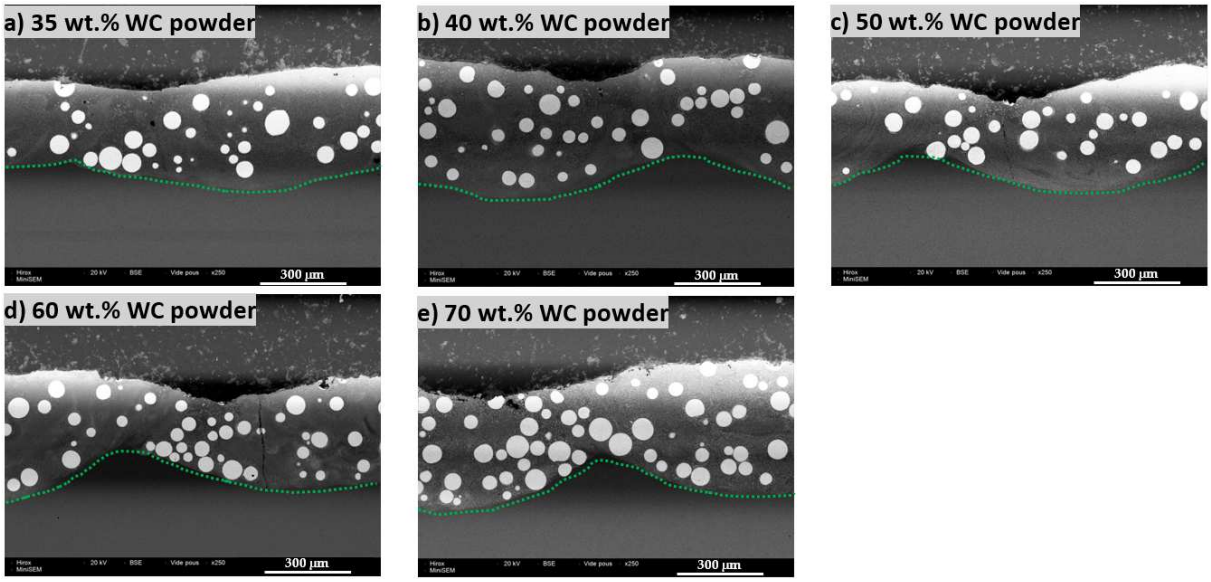

Figure 5: SEM micrographs (BSE) in section of the LC coatings obtained from mixtures of the NiCrBSi matrix (11 wt% Cr) with different carbide contents a) 35 wt%, b) 40 wt%, c) 50 wt%, d) 60 wt% and e) 70 wt%.

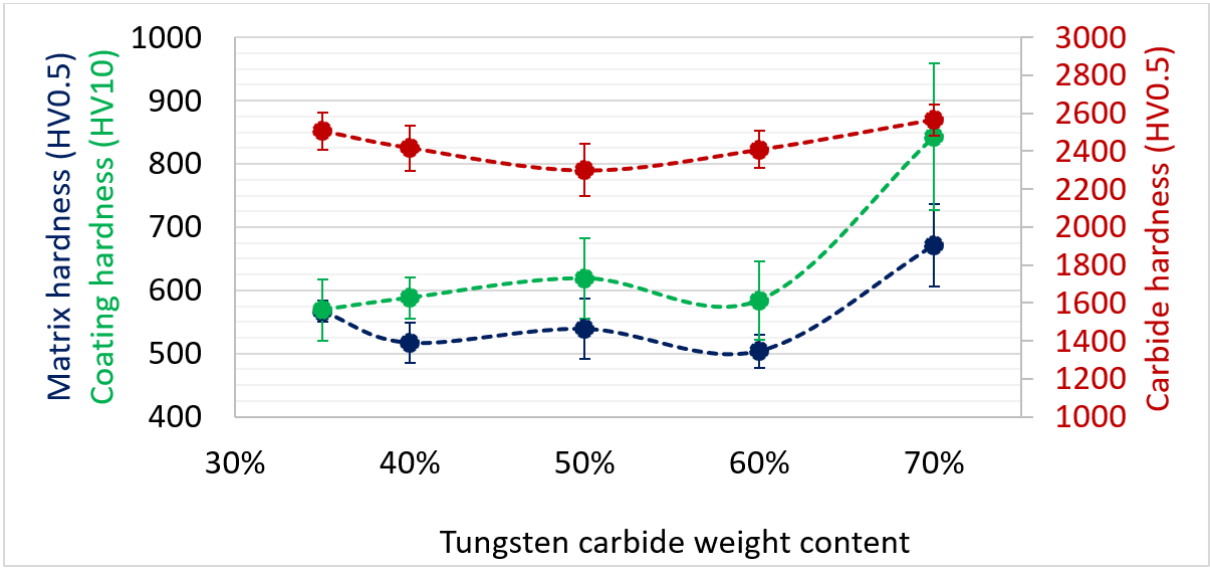

Figure 6: Effect of the tungsten carbide content in the powder mixture deposited by LC on the hardness of the NiCrBSi matrix (blue), the carbides red) and the coating (green).

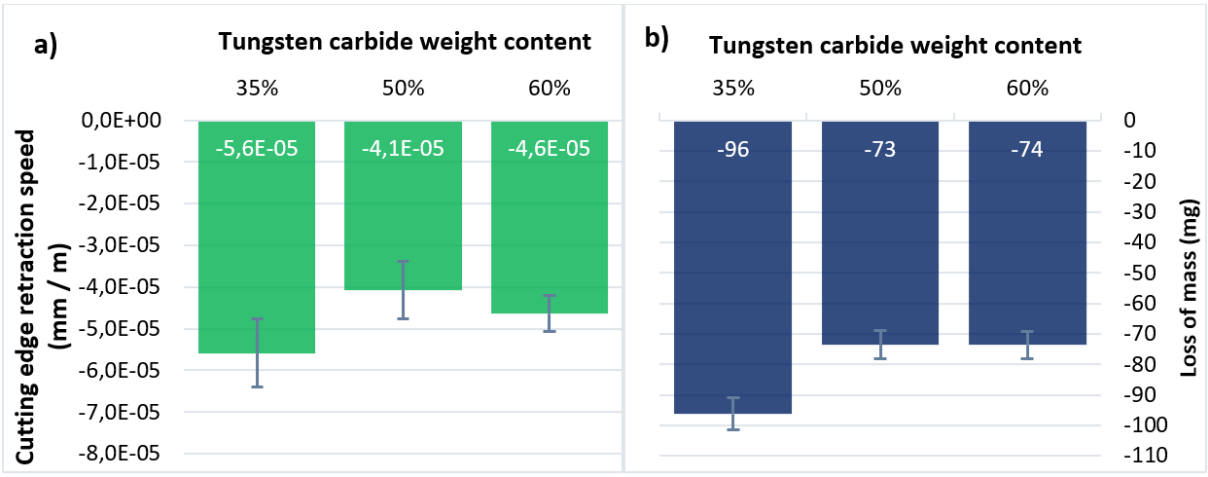

Figure 7: Effect of WC content in the powder deposited by LC on the cutting performance of plants (cutting test).

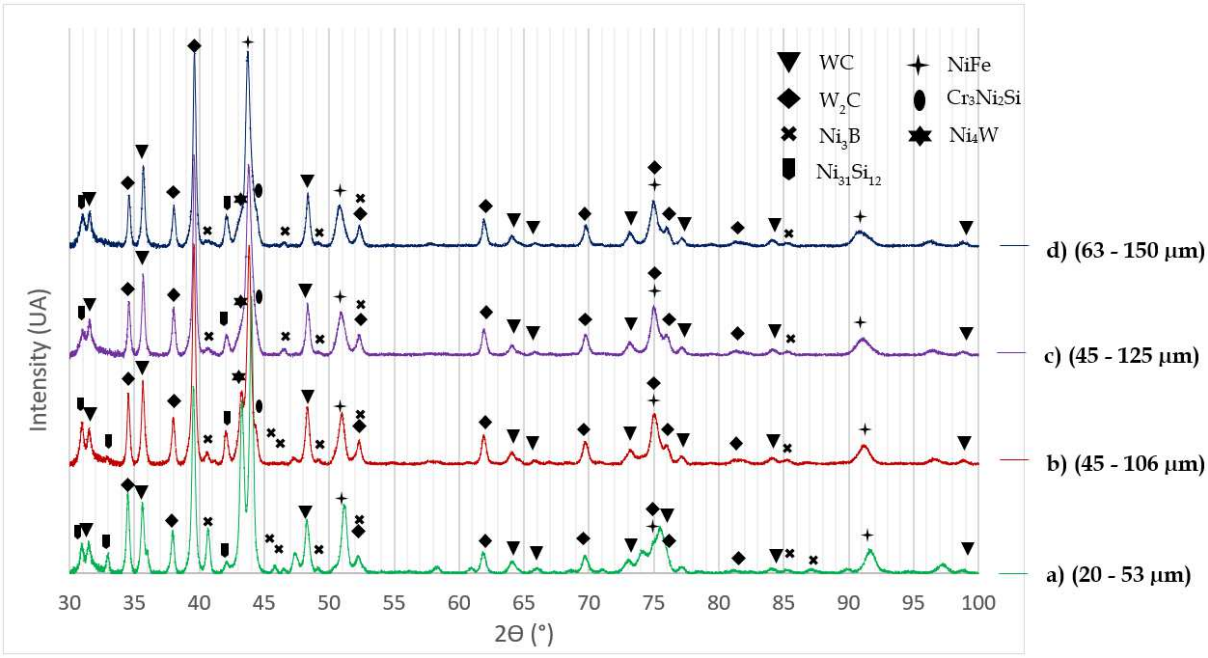

Figure 8: Diffractograms of coatings deposited by LC from powder mixtures with the NiCrBSi matrix (11 wt% Cr) reinforced with 60 wt% of WC tungsten carbide powder with different particle sizes.

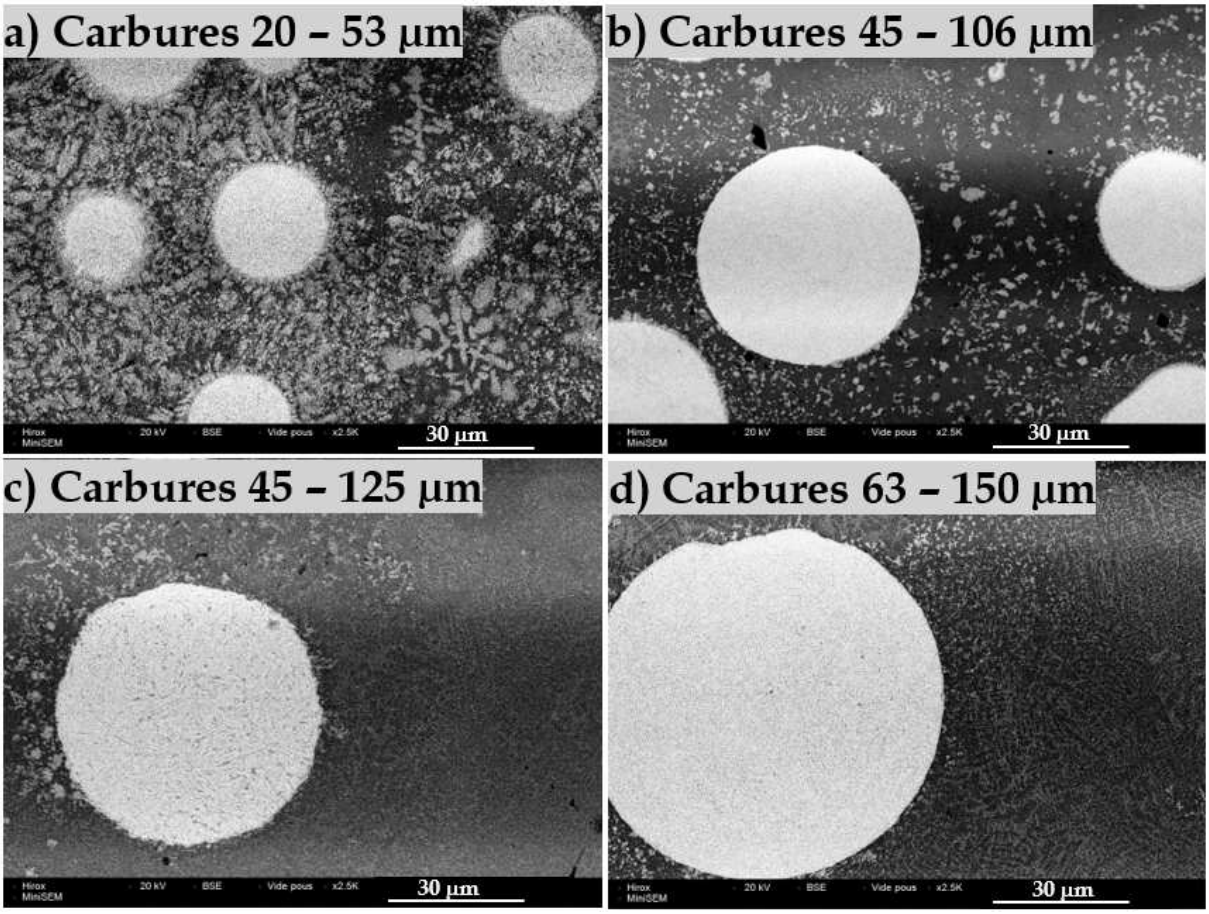

Figure 9: Cross section SEM micrographs (BSE) of coatings deposited by LC from mixtures of 40 wt% of NiCrBSi with 60 wt% of carbide powder with different particle sizes a) 20 - 53 µm, b) 45 - 106 µm, c) 45 - 125 µm and d) 63 - 150 µm.

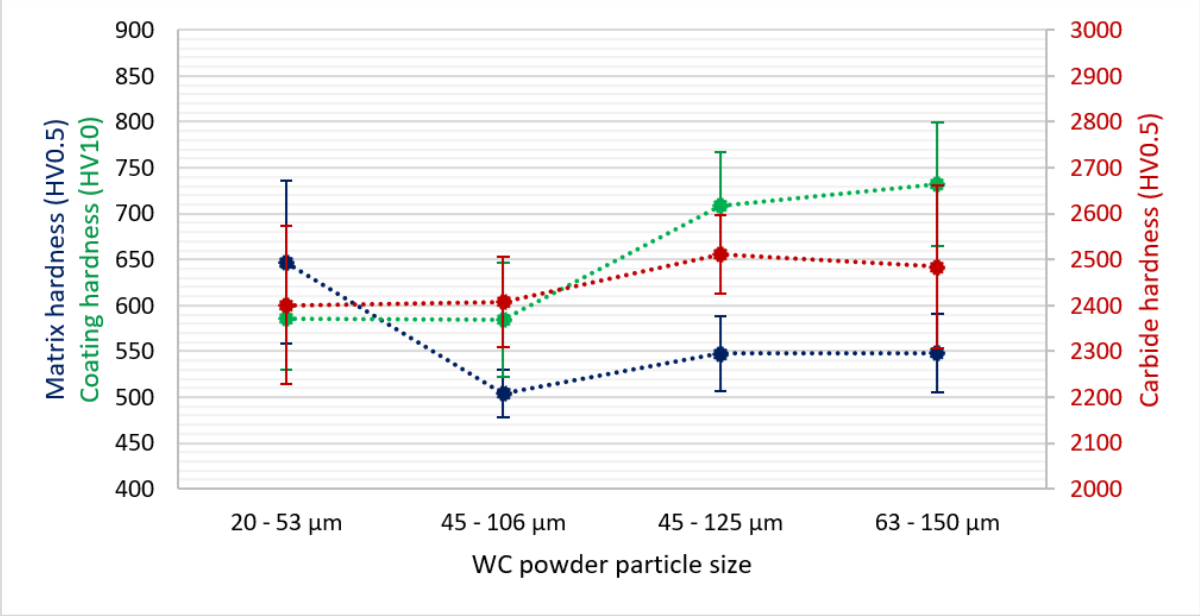

Figure 10: Effect of the particle size of tungsten carbide powder deposited by LC on the hardness of the NiCrBSi matrix (blue), the carbides (red) and the coating (green).

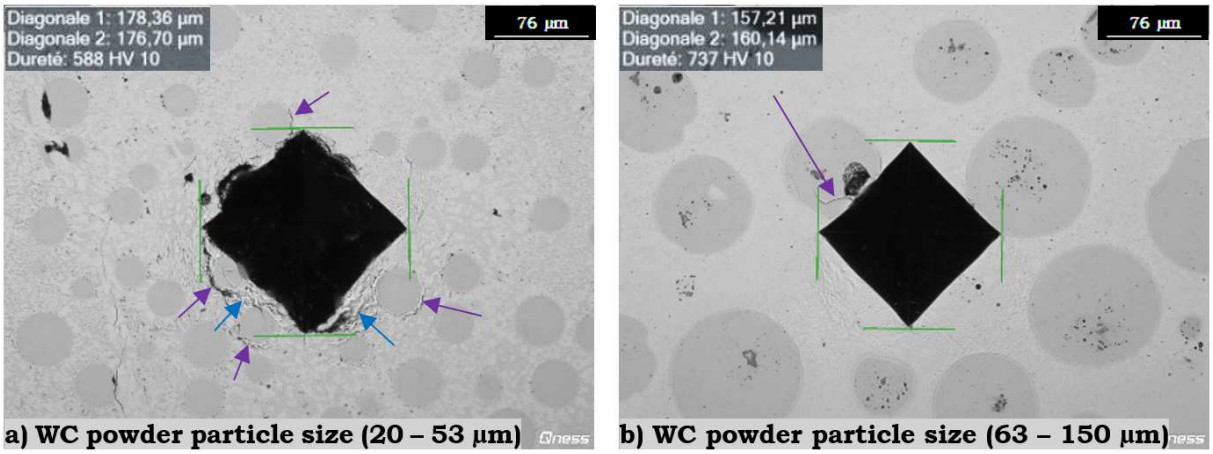

Figure 11: Hardness imprints on the polished surface of coatings deposited by LC from the mixture of the NiCrBSi matrix with 60 wt% of WC carbide powder with different particle sizes a) 20 - 53 µm and b) 63 - 150 µm

.

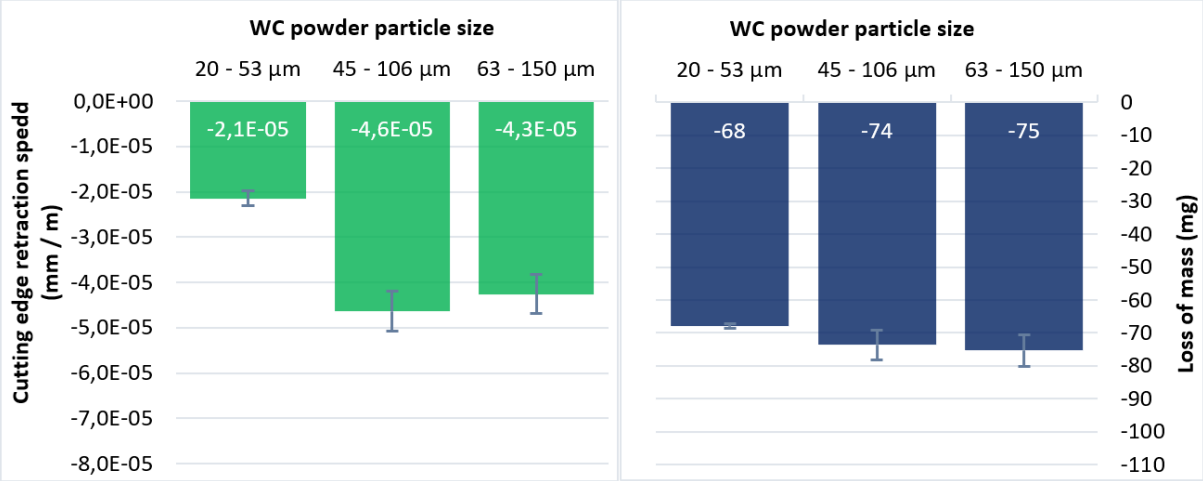

Figure 12: Effect of the particle size of the WC tungsten carbide powder mixed with 40 wt% of NiCrBSi matrix, deposited by LC, on the cutting performance of plants (cutting test).